Supplementary Information (SI) for Journal of Materials Chemistry B.

Insight into the induced performance of 1-phenylethyl segment in aza-BODIPY system

Yufei Xiao,[‡,a] Xiaoyan Gao,[‡,b,d] Yunsheng Xue,[c] Xin-Dong Jiang,*[a] Gaowu Qin*[a] and Xiaohong Sun*[b,d]

[a]Institute for Strategic Materials and Components, Liaoning & Shenyang Key Laboratory of Functional Dye and Pigment, Shenyang University of Chemical Technology, Shenyang, 110142, China. E-mail: xdjiang@syuct.edu.cn, gwqin@syuct.edu.cn

[b]Department of Neurology, the Fourth Affiliated Hospital of China Medical University, Shenyang, *110032*, China. Email: xhsun@cmu.edu.cn

[c]Jiangsu Key Laboratory of New Drug Research and Clinical Pharmacy, School of Pharmacy, Xuzhou Medical University, Jiangsu, China.

[d]Science Experiment Center, China Medical University, Shenyang, China.

[‡]These authors contributed equally to this work.

1 Experimental section

1.1 General

Unless otherwise stated, all chemical substances and organic solvents used were analytical grade and obtained from Energy Chemical & Technology (Shanghai) Co. Ltd. without extra purification. A VARIAN Mercury 400 MHz spectrometer was employed to record ^1H NMR spectra. Chemical shifts in ^1H NMR (δ) are presented in ppm downfield from Me_4Si, as estimated by residual chloroform (δ 7.26 ppm). On a VARIAN Mercury 125 MHz spectrometer, ^{13}C NMR spectra were recorded in $CDCl_3$, reported in ppm with the internal chloroform signal at δ=77.0 ppm as the reference. The precise molecular weight of the product is determined utilizing a high resolution mass spectrometer. A UV-2550 spectrophotometer was used to record an absorption spectroscopy at 298 K. Fluorescence spectra are presented as cm^{-1} and were captured using an F-128 spectrophotometer. Laser particle size analyzer was bought from Malvern. The temperature of the solution is tracked by a temperature determining camera. The light source employed for light irradiation was a 808 nm laser that was purchased from Changchun New Industries Optoelectronics Technology and controlled by a fiber linked laser system for the laser output power. A CEL-NP 2000 power meter was implemented for evaluating the optical power density which was obtained from Beijing Zhong Jiao Jin Yuan Technology Co, Ltd. In the CCK8 assessment, a BioTek Synergy H1 microplate reader was utilized. Fluorescence imaging was estimated using an Olympus Confocal Laser Fluorescence Microscope FV1200 (Japan). The flow cytometric analysis was used the BD FACSVerse™ Flow Cytometer.

1.2 Singlet Oxygen Detection

The $^1O_2$ production in toluene was determined utilizing 1,3-diphenylisobenzofuran (DPBF) as a $^1O_2$ trap. The absorbance of DPBF at 416 nm was adjusted to about 1.1 in toluene and the absorbance of the dyes was adjusted to about 0.7 at 620 nm. The 635 nm laser light was used for the excitation of the dye, the optical radiation power was 0.3 W/cm^2, and the illumination time was 0-20 min. Methylene blue (MB) was used as a reference (Φ_Δ = 57% in toluene).

The $^1O_2$ production efficiency of the dyes was calculated from the decrease of absorbance of DPBF (monitored at 416 nm) according to the following equation:

$$\Phi_{\mathrm{sam}} = \Phi_{MB}(\frac{m_{sam}}{m_{MB}})(\frac{F_{MB}}{F_{sam}})$$

Where “sam” represents the dye with unknown $^1O_2$ quantum yield and “MB” represents the reference methylene blue. “m” is the slope of DPBF absorption peak decline, “F” is the absorption correction factor, F = $1\text{-}10^{\text{-O.D.}}$. O.D. represents the absorption value of the sample at the wavelength of light radiation.

1.3 Photothermal effect and efficiency

A variety of concentrations were created (0-80 μM), and all of them were exposed to 0.8 W/cm^2 of an 635 nm laser for 5 min. The temperature was measured every 30 s using an infrared thermal imaging camera. Meanwhile, 30 μM dye was treated by 635 nm laser at various power densities (0.2-0.8 W/cm^2) for 5 min. The temperature was collected by the infrared thermal imaging camera every 30 s. The solution was cooled following 5 min of light irradiation. During this process, the solution temperature was monitored every 30 s. The photothermal conversion efficiencies (η) was calculated using the following method.

$$\eta = \frac{hs(T_{Max} - T_{Surr}) - Q_{Dis}}{I(1 - 10^{-A})}$$

h means heat transfer coefficient, *s* was for container surface area, Q_{Dis} stands for heat dispersed from the laser via the solvent and container, *I* was for laser power, and *A* represents for absorbance at excitation wavelength. η denotes photothermal conversion efficiency.

$$hs = \frac{mC}{\tau_s}$$

m is the total quantity of the photothermal reagent containing solution, *C* represents the temperature coefficient, and τ_s is the relevant time constant.

$$t = -\tau_s ln(\theta)$$

The temperature of the driving force is a non-dimensional parameter termed *θ*.

$$\theta = \frac{T - T_{Surr}}{T_{Max} - T_{Surr}}$$

T is the current temperature, T_{Max} is the highest steady state temperature, and T_{surr} denotes the surrounding temperature.

1.4 Computational method

All calculations have been performed by using the Gaussian 09 programs [1]. Geometrical structures were optimized using the DFT method with the dispersion-inclusive hybrid functional D3-B3LYP [2-4] and 6-31G(d,p) basis set. Vibrational frequencies were calculated at the same level to characterize the stationary point as minima points. The vertical transition energies were calculated using the TDDFT method with D3-B3LYP and 6-31+G(d,p) basis set. Solvent effects were simulated using the polarizable continuum model (PCM) [5, 6].

1.5 The Preparation of dye-nanoparticles

Nano-deposition method was used for preparation. 1 ml THF solution containing 1 mg dye and 5 mg DSPE-PEG$_{2000}$ is slowly but steadily injected to the 10 ml aqueous solution. Following that, THF was volatilized by constant stirring for 24 h to ensure that dye was evenly spread in the solution. By centrifuging the appropriate NPs at 6000 rpm for 5 min, the final produces could be attained.

1.6 Cell culture

Human glioblastoma U251 cells were used for in vitro experimentation. U251 cells were cultured in Dulbecco's Modified Eagle's Medium (DMEM) high glucose, and supplemented with 10% fetal bovine serum (FBS), 1% penicillin/streptomycin. The cells were cultured in a relatively humidified atmosphere at 37 °C with 5% CO$_2$. The cells were divided into four groups: control group (no treatment), the light group (635nm laser irradiation treatment), NPs group (20 μM **PE-BDP** NPs treatment) and NPs + light (20 μM **PE-BDP** NPs+ 635nm laser irradiation treatment).

1.7 CCK8 assay

The U251 cells (6 × 10^3/well) were seeded into 96-well plates and incubated overnight, then incubated with different concentrations of **PE-BDP** NPs (0, 1, 10, 15, 20, 30 and 40 μM) for 24 h. Subsequently, the light group cells were treated with 635 nm laser irradiation for 5 min every well. The medium replaced with DMEM medium containing Cell Counting Kit-8 (CCK8, APExBIO, Cat#K1018) reagent and cells were incubated for 2 h. The absorbance at 450 nm was determined through a microplate reader (BioTek, Santa Clara, VT, USA) and cell viability was normalized to the matched control group.

1.8 Colony formation assay

A total of 1x10^3 cells was seeded to each well of 6-well plates, shaken, mixed, and cultured in a relatively humidified atmosphere at 37 °C with 5 % CO_2. Four different treatments divided the cells into four groups. Upon colony formation, the colonies were fixed with 4% paraformaldehyde for 30 min, subsequently stained with 0.5% crystal violet, photographed after rinsing.

1.9 EdU-488 assay

EdU cell Proliferation kit with Alexa Fluor 488 (Beyotime, Cat#C0071S) was performed to estimate cell proliferation. Briefly, four groups of U251 cells were incubated with EdU working solution for 2 h according to the product manual. Then being fixed with 4% paraformaldehyde and permeabilized with 0.5% Triton X-100. Subsequently, cells were labeled with click reaction, and DAPI was used to stain the nuclei. The cells were captured by fluorescence microscopy and analyzed by ImageJ software (NIS, USA).

1.10 Transwell migration assay

The treated U251 cells (2× 10^4 per well) were plated with 200 μL serum-free DMEM medium to the upper transwell chamber, and 600 μL DMEM medium containing 20% fetal bovine serum was added to the lower chamber, respectively. After incubation for 24 h, the cells were fixed using 4% paraformaldehyde and then subjected to staining using 0.1% crystal violet. Images were captured using a microscope (Olympus, IX51, Japan).

1.11 Wound healing assay

Four groups of treated U251 cells were seeded in 24-well plates and incubated to 100% confluence. Subsequently, controlled wounds were created vertically using a 200 μL pipette tip and debrises were washed off with PBS. The cells were incubated with serum-free DMEM high glucose medium and captured photograph under a microscope (Olympus, IX51, Japan) at 0 h, 12 h and 24 h after scratching. Finally, the wound healing area was measured with ImageJ software (NIH).

1.12 Calcein AM staining assay

The Calcein AM staining kit (Beyotime, Cat#C1367M) was employed to assess cells survival rate. U251 cells were plated in 96-well plates, after culturing 24 h, divided into four different groups as before treatment. Subsequently, cells were incubated with 1 μM Calcein AM in the well of plate for 20 min and Hoechst 33342 was used to stain the nuclei. The cells were photographed under a fluorescence microscope and analyzed by ImageJ software (NIS, USA).

1.13 TUNEL assay

Fluorometric TUNEL System (Promega, Cat#G3250) was employed to detect apoptosis level from four different groups of U251 cells. The cells were incubated with a mixture solution of TDT enzyme, dUTP, and buffer, then DAPI was used to stain the nuclei. The cells were captured under a fluorescence microscope.

1.14 ROS assay

Reactive oxygen species (ROS) probe DCFH-DA (Wuhan Servicebio Technology Co., Ltd) was employed to evaluate the intracellular ROS levels from four different groups of U251 cells. The cells were stained with 20 μmol/L DCFH-DA solution for

30 min in the dark environment. After washing with PBS, the cells were photographed under a fluorescence microscope. Further, the fluorescence intensity of DCFH-DA was measured by ImageJ software (NIS, USA).

1.15 Statistical analysis

Data was expressed as mean ± standard deviation (SD). Comparison of means among groups was performed using one-way analysis of variance (ANOVA) followed by Tukey's multiple comparisons test. All data statistical analyses were performed using GraphPad Prism software 9.0 (San Diego, CA, USA). $p < 0.05$ was considered significant.

2 Synthesis

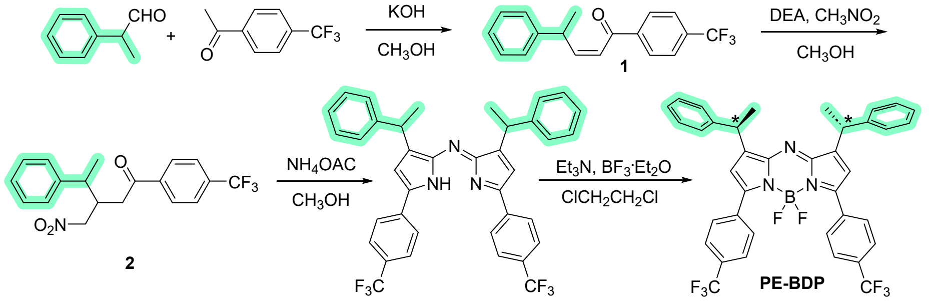

Synthesis of 1

Under air, 2-phenylpropionaldehyde (2 mL, 14.8 mmol) was added to *p*-trifluoromethylacetone (2.8 g, 14.8 mmol) in 50 mL methanol. Then, 2 g KOH in 2 mL H_2O was added to the mixture, and this mixture was refluxed for 24 h. After cooling to room temperature, the mixture was extracted with CH_2Cl_2 (2 × 50 mL), and the organic layer was washed with brine (2 × 100 mL) and dried over anhydrous Na_2SO_4. The solvents were removed by evaporation, and the resulting crude mixture was separated by column chromatography (CH_2Cl_2/*n*-hexane =2:3) to afford dye **1** as yellow solid powder (2.9 g, 9.53 mmol, 64%). ^{1}H NMR (400 MHz, $CDCl_3$): δ (ppm) 8.07 (d, ^3J = 8.0 Hz, 2H), 7.71 (d, ^3J = 8.0 Hz, 2H), 7.38 (d, ^3J = 8.0 Hz, 2H), 7.28 (t, ^3J = 8.0 Hz, 2H), 7.19-7.25 (m, 3H), 3.89 (d, ^3J = 8.0 Hz, 1H), 2.08-2.11 (m, 3H). ^{13}C NMR (125 MHz, $CDCl_3$): δ (ppm) 196.9, 143.1, 139.5, 138.8, 128.7, 128.5, 128.3, 127.8, 127.3, 125.9, 125.8, 118.9, 25.7, 16.5.

Synthesis of 2

Under air, diethylamine (5 mL) and nitromethane (4 mL) were added to compound **1** (2.9 g, 9.53 mmol) in anhydrous methanol (40 mL). The mixture was refluxed for 24 h. After cooling to room temperature, the mixture was extracted with CH_2Cl_2 (2 × 50 mL), and the organic layer was washed with brine (2 × 100 mL) and dried over anhydrous Na_2SO_4. The solvent was removed under reduced pressure, and resulting crude mixture was separated by column chromatography (CH_2Cl_2:*n*-hexane = 1:2) to afford compound **2** (3.1 g, 8.49 mmol, 89%) as yellow solid powder. ^{1}H NMR (400 MHz, $CDCl_3$): δ (ppm) 7.90 (d, ^3J = 8.0 Hz, 2H), 7.65 (t, ^3J = 8.0 Hz, 2H), 7.12-7.29 (m, 5H), 4.62 (dd, ^3J = 12.0, 5.6 Hz, 1H), 4.31 (dd, ^3J = 12.0, 5.6 Hz, 2H), 3.09-3.12 (m, 2H), 1.33 (d, ^3J = 6.8 Hz, 1H), 1.25 (d, ^3J = 6.8 Hz, 3H). ^{13}C NMR (125 MHz, $CDCl_3$): δ (ppm) 197.3, 143.3, 139.2, 129.1, 128.7, 128.4, 127.6, 127.3, 125.9, 125.5, 40.2. 39.6, 37.5, 26.8, 18.5.

Synthesis of dye PE-BDP

NH_4OAc (20 g, 259.4 mmol) was added to compound **2** (3.1 g, 8.49 mmol) in anhydrous methanol (50 mL). The mixture was refluxed for 24 h. After cooling to room temperature, the mixture was extracted with CH_2Cl_2 (3 × 50 mL), and the organic layer was washed with brine (3 × 50 mL) and dried over anhydrous Na_2SO_4. After the solvent was removed under reduced pressure, and resulting crude mixture was separated by column chromatography (CH_2Cl_2: *n*-hexane =3:1) to afford the precursor (3.5 g, 5.45 mmol) as blue solid powder. This precursor was dissolved in 30 mL anhydrous $ClCH_2CH_2Cl$. Triethylamine (0.5 ml, 3.6 mmol) was added and stirred at room temperature for 30 min, followed by dropwise addition of $BF_3{\cdot}Et_2O$ (1 mL, 7.9 mmol) with stirring at room temperature for 30 min. The mixture was then heated in 70 °C for 4 h. After cooling to room temperature, the mixture was extracted with CH_2Cl_2 (2 × 50 mL), and the organic layer was washed with brine (2 × 50 mL) and dried over anhydrous Na_2SO_4. After solvent removal by evaporation, and the resulting crude product was separated by column chromatography (CH_2Cl_2/*n*-hexane = 3:2) to afford dye **PE-BDP** (2.1 g, 3.04 mmol, 35%) as a blue solid powder. ^{1}H NMR (400 MHz, $CDCl_3$): *δ* (ppm) 8.01 (d, ^3J = 8.0 Hz, 4H), 7.67 (d, ^3J = 8.0 Hz, 4H), 7.31-7.36 (m, 10H), 6.61 (s, 1H), 6.57 (s, 1H), 4.53 (q, ^3J = 7.2 Hz, 2H), 1.73 (d, ^3J = 7.2 Hz, 3H), 1.71 (d, ^3J = 7.2 Hz, 3H). ^{13}C NMR (125 MHz, $CDCl_3$): δ (ppm) 158.45, 153.6, 145.7, 144.2, 134.5, 129.6, 128.6, 127.4, 126.6, 125.4, 124.5, 122.7, 120.2, 29.6, 21.3. HRMS (ESI) m/z calcd for $C_{38}H_{29}BF_8N_3^+$ $(M+H)^+$ 690.23213, found 690.23242.

3 NMR and HRMS

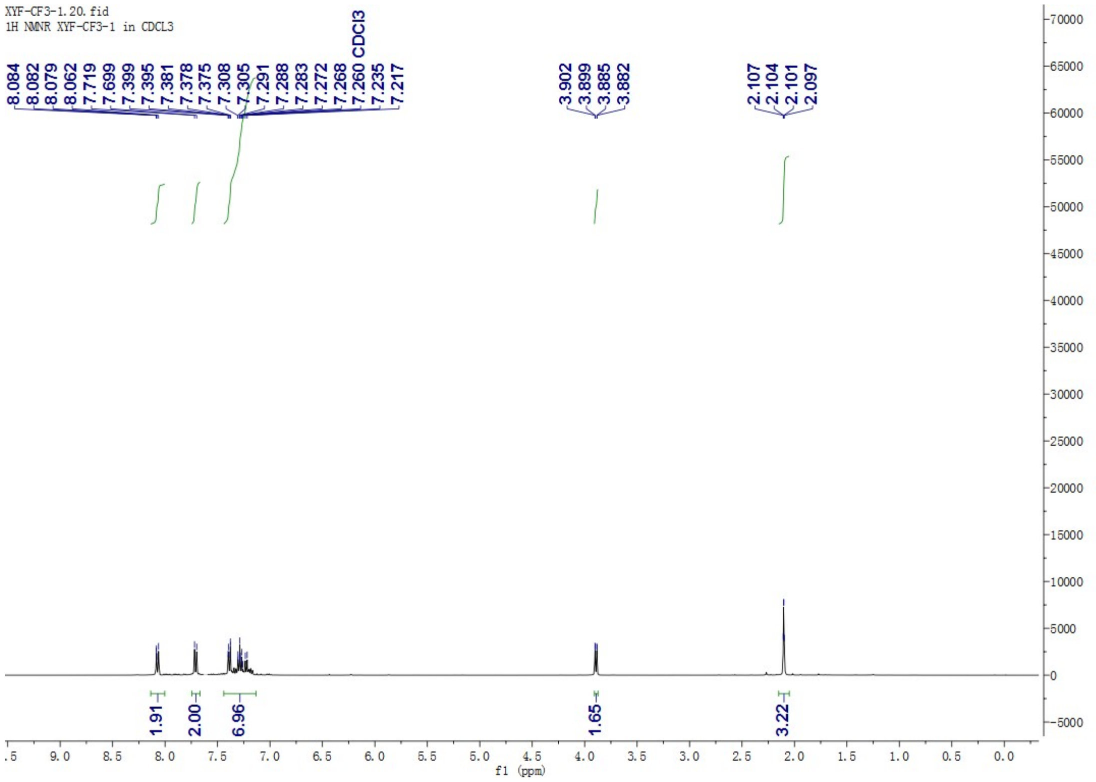

^{1}H NMR of **1**

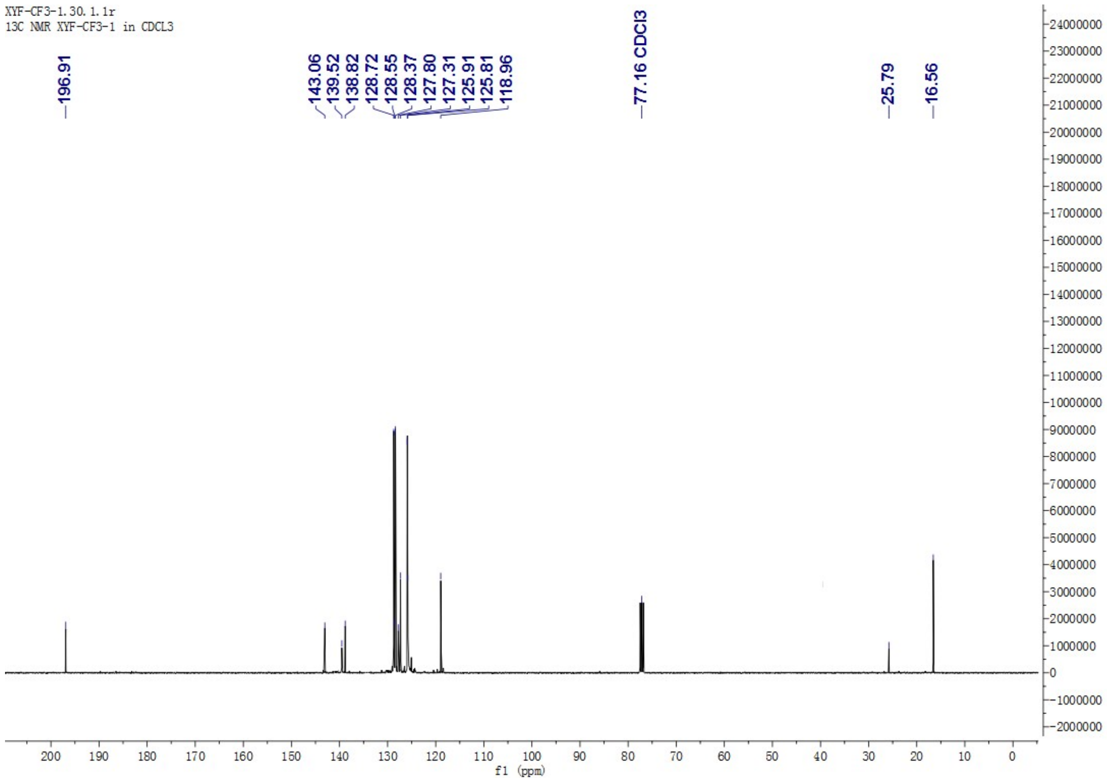

^{13}C NMR of **1**

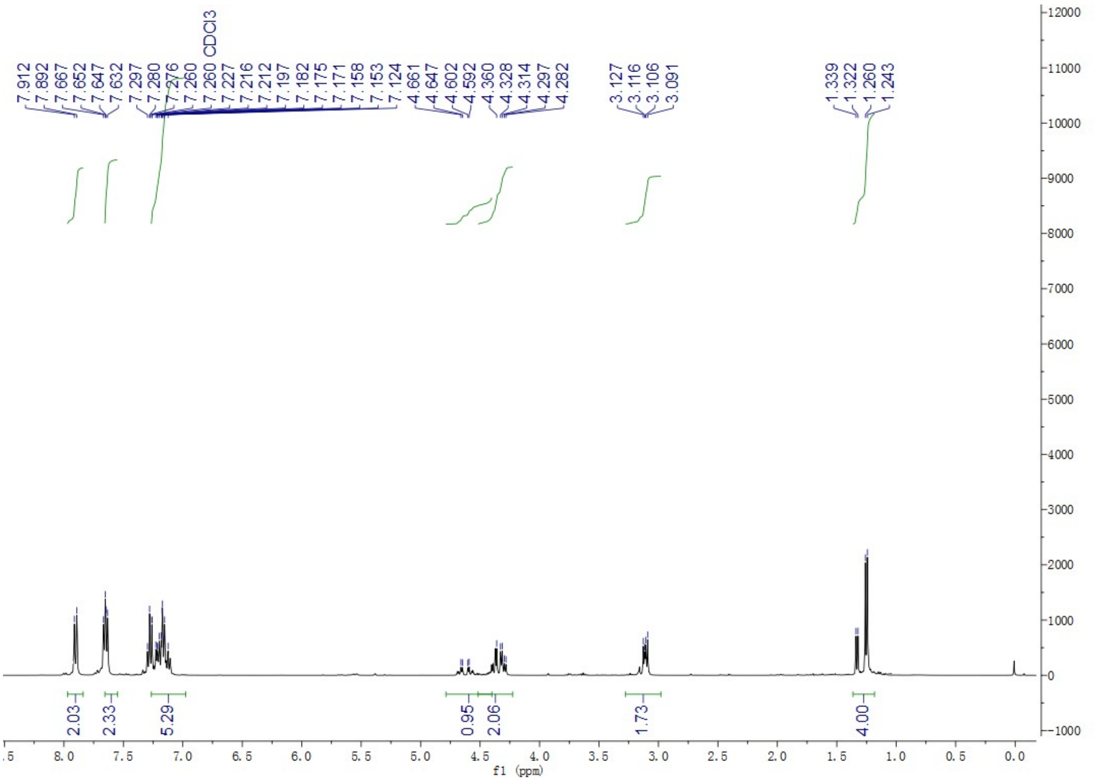

^{1}H NMR of **2**

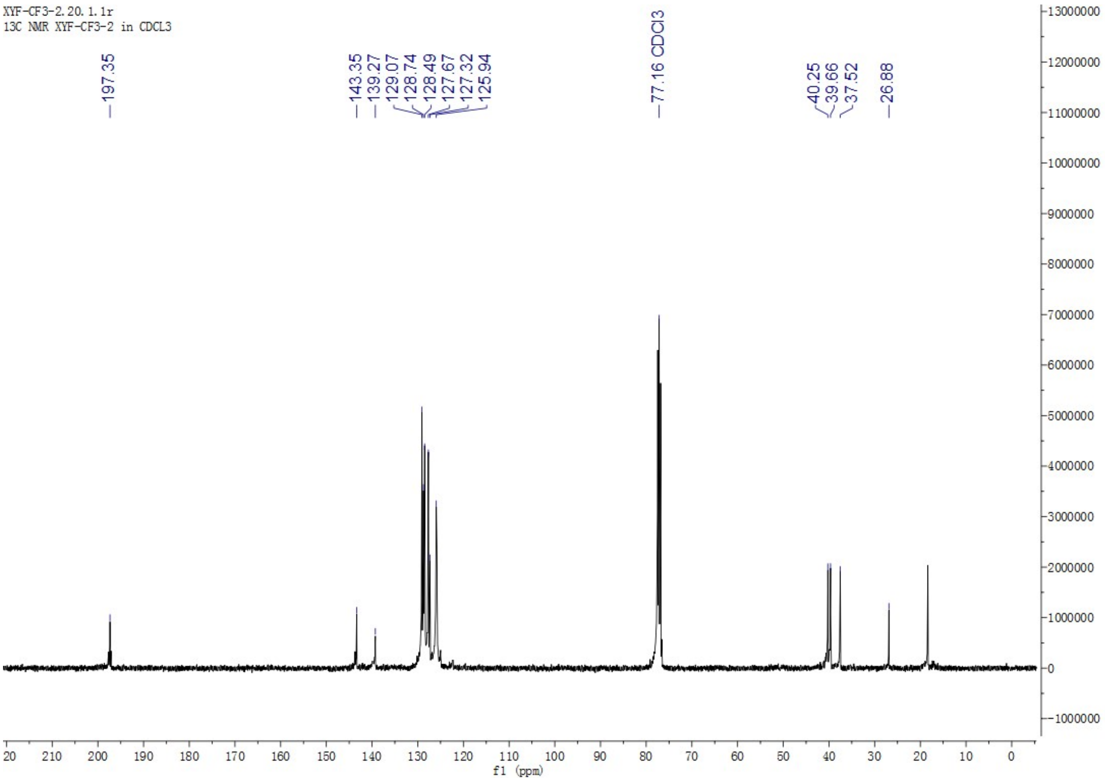

^{13}C NMR of **2**

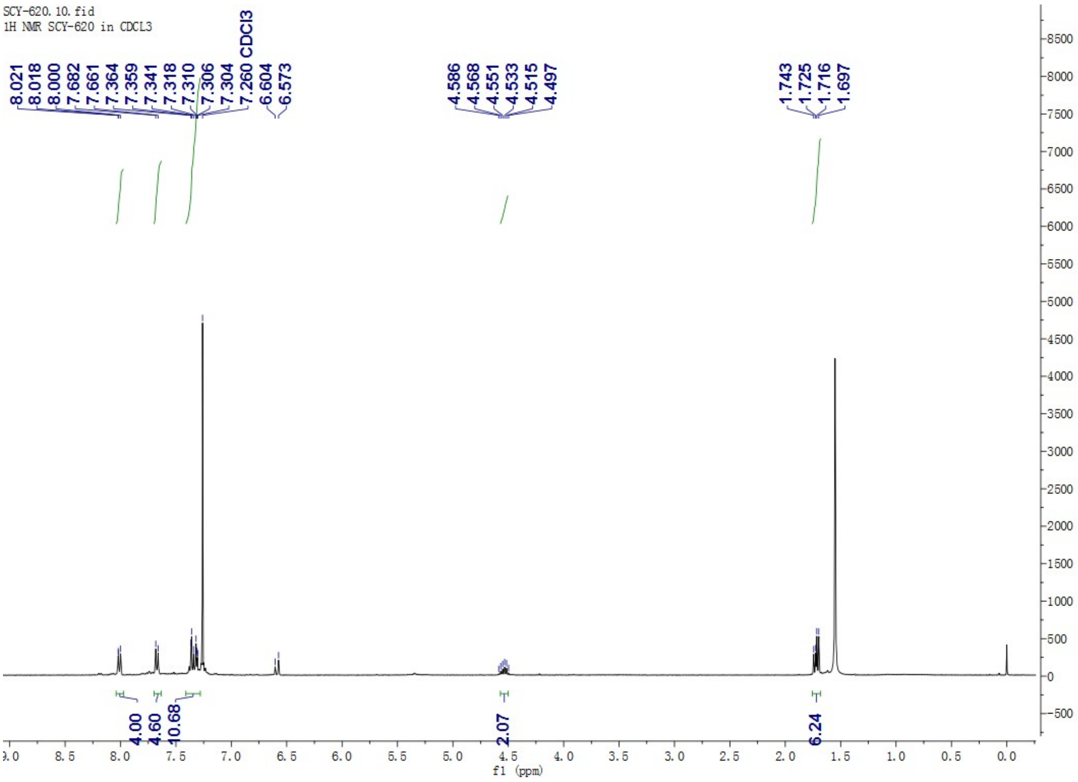

^{1}H NMR of **3**

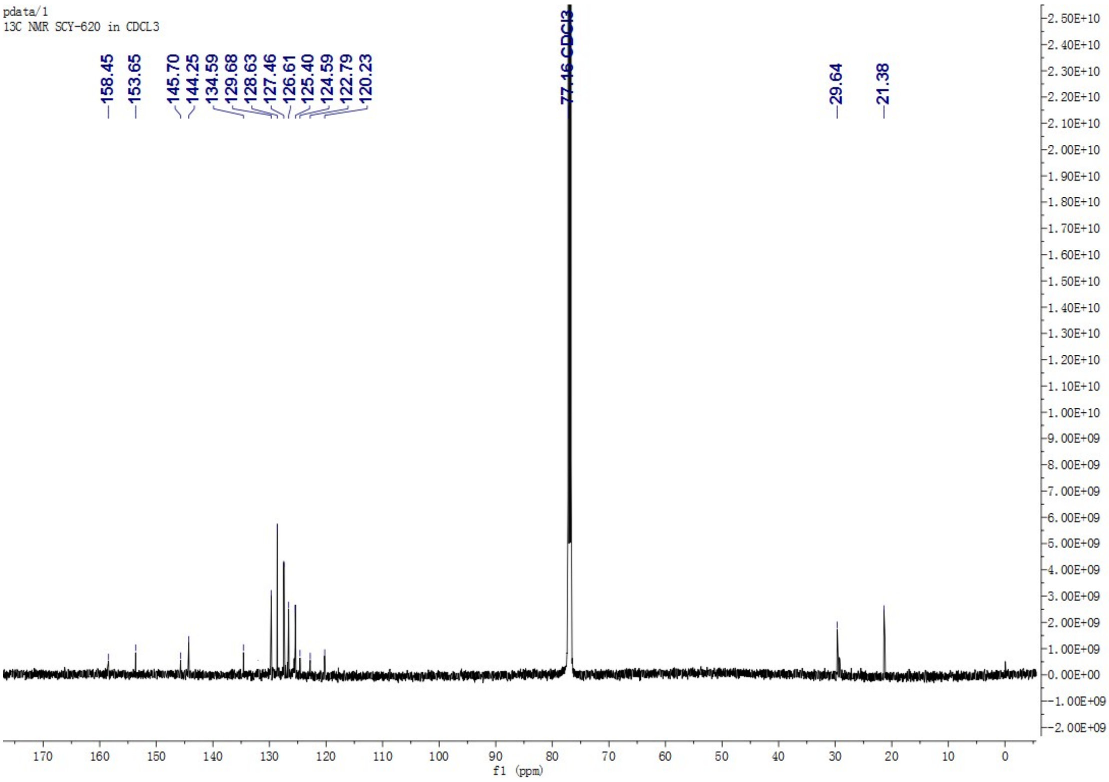

^{13}C NMR of **3**

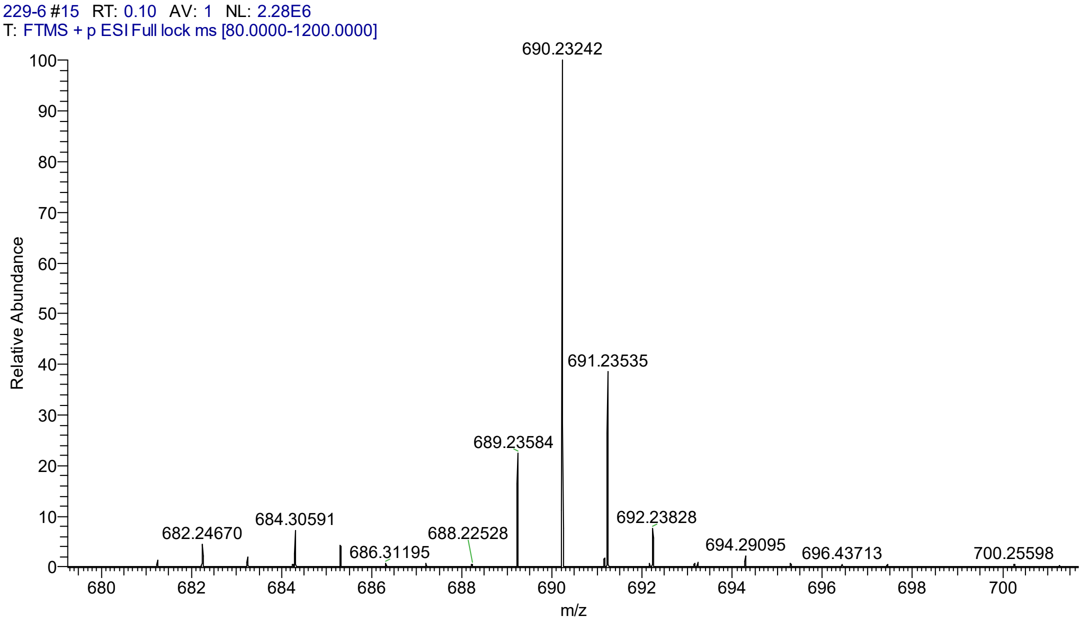

PE-BDP: HRMS (ESI) m/z calcd for $C_{38}H_{29}BF_8N_3^+$ $(M+H)^+$ 690.23213, found 690.23242.

4 Figure and Table

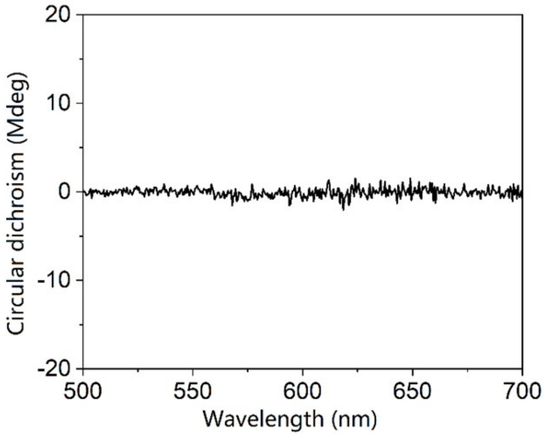

Fig. S1 CD spectra of **PE-BDP**.

Fig. S2 Photos of **PE-BDP** in different solvents.

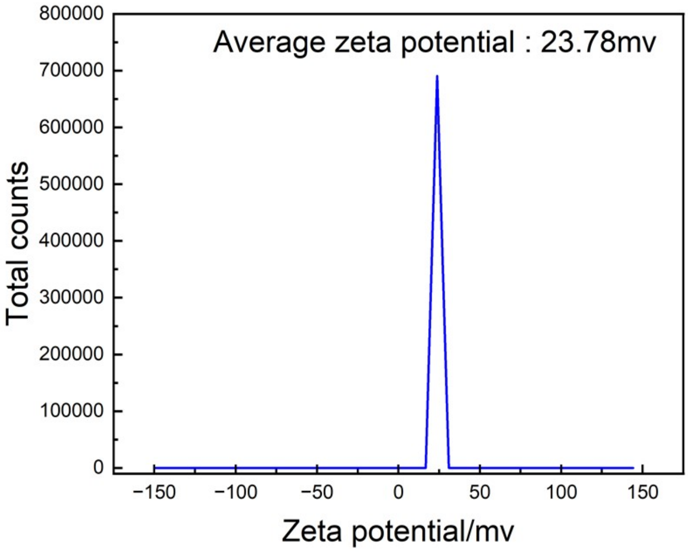

Fig. S3 The zeta potential of **PE-BDP NPs.**

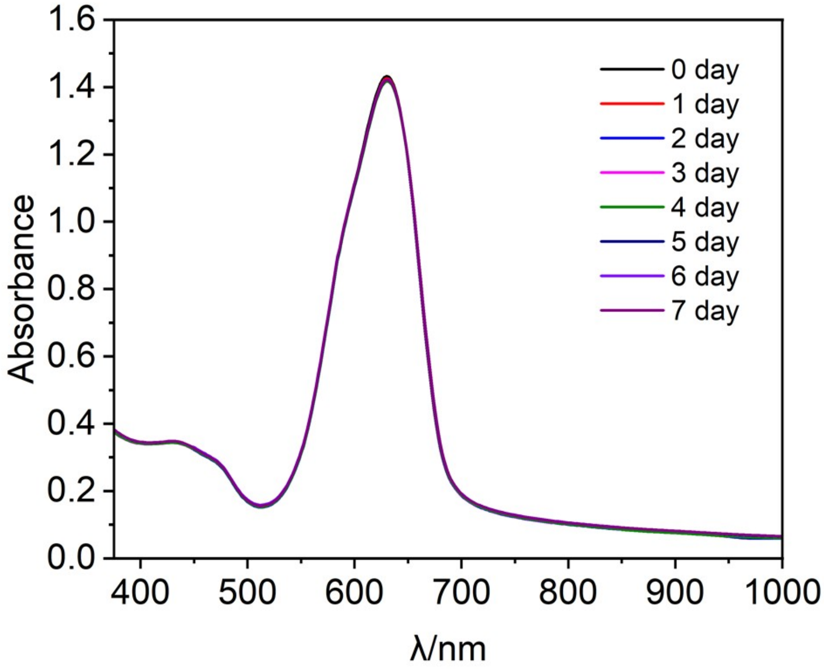

Fig. S4 The stability of **PE-BDP NPs.**

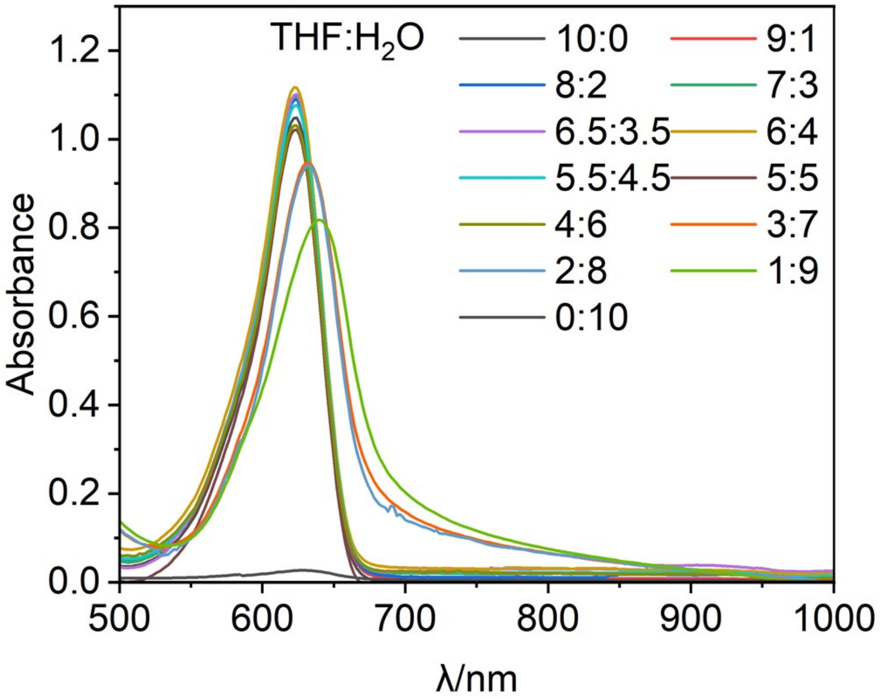

Fig. S5 The absorption spectra of **PE-BDP** in different solvent ratios (THF:H_2O).

Table S1 Photophysical properties of **PE-BDP** in various solvents at 298 K.

	PE-BDP			
Solvent	λ_{abs} (nm)/λ_{em} (nm)	FWHM	Stokes shift	Φ_f
DCM	620/657	42	37	0.23
ACN	614/653	42	39	0.21
EtOAc	618/654	41	36	0.22
DMF	624/660	41	36	0.16
DMSO	626/663	43	37	0.13
Toluene	624/660	42	36	0.22
THF	622/658	41	36	0.21
n-hexane	618/651	40	33	0.24

Dye	HOMO	LUMO	ΔE(LU-HO)
PE-BDP	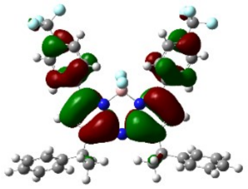	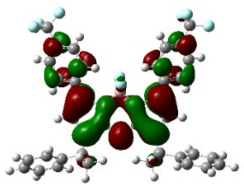	
	-5.7163	-3.4033	2.31
PE-BDP-anion	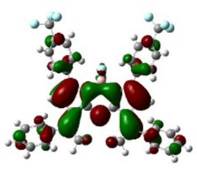	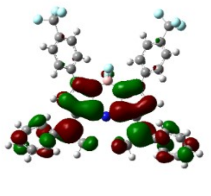	
	-5.3731	-3.1252	2.25

Fig. S6 Frontier molecular orbital profiles and energies (eV) of the studied species.

Table S2 Calculated maximum absorption wavelength $\lambda_{max,ab}$ (eV, nm), oscillator strength (f) and transition assignment.

Molecule	*E* (eV)	$\lambda_{max,ab}$ (nm)	*f*	Assignment	Exp. (nm)
PE-BDP	2.1881	566.63	0.8447	HOMO→LUMO	620
PE-BDP-anion	2.1804	568.63	0.6140	HOMO→LUMO	672

Table S3 Excitation energies (eV) of the low-lying excited states based on the optimized S_0-geometries of the studied compounds.

COMP	**S1**	**T1**	**T2**	**ΔE_{S-T}**
PE-BDP	2.1881	0.8959	2.4030	1.2922
PE-BDP-anion	2.1804	1.2243	1.8366	0.3438

5 X-ray data for PE-BDP

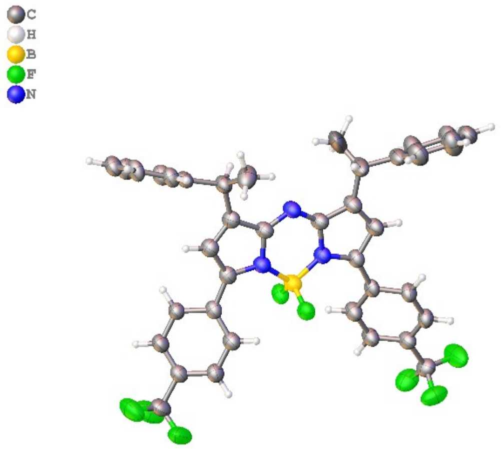

SCY-CF3

Table 1 Crystal data and structure refinement for SCY-CF3.

Identification code	SCY-CF3
Empirical formula	$C_{38}H_{28}BF_8N_3$
Formula weight	689.44
Temperature/K	159(15)
Crystal system	triclinic
Space group	P-1
a/Å	10.0274(14)
b/Å	13.452(2)
c/Å	14.1617(19)
α/°	115.638(14)
β/°	98.781(11)
γ/°	104.759(13)
Volume/Å^3	1587.9(4)
Z	2
ρ_{calc}g/cm^3	1.442
μ/mm^{-1}	1.005
F(000)	708.0
Crystal size/mm^3	0.15 × 0.14 × 0.12
Radiation	Cu Kα (λ = 1.54184)
2Θ range for data collection/°	7.262 to 133.192
Index ranges	$-11 \leq h \leq 11$, $-16 \leq k \leq 12$, $-10 \leq l \leq 16$
Reflections collected	10532
Independent reflections	5546 [R_{int} = 0.1245, R_{sigma} = 0.1707]
Data/restraints/parameters	5546/429/454
Goodness-of-fit on F^2	1.025
Final R indexes [I>=2σ (I)]	R_1 = 0.0919, wR_2 = 0.2388

Final R indexes [all data] $R_1 = 0.1824$, $wR_2 = 0.3108$

Largest diff. peak/hole / e Å^{-3} 0.62/-0.42

Crystal structure determination of [SCY-CF3]

Crystal Data for $C_{38}H_{28}BF_8N_3$ (M =689.44 g/mol): triclinic, space group P-1 (no. 2), a = 10.0274(14) Å, b = 13.452(2) Å, c = 14.1617(19) Å, α = 115.638(14)°, β = 98.781(11)°, γ = 104.759(13)°, V = 1587.9(4) Å^3, Z = 2, T = 159(15) K, μ(Cu Kα) = 1.005 mm^{-1}, $Dcalc$ = 1.442 g/cm^3, 10532 reflections measured (7.262° ≤ 2Θ ≤ 133.192°), 5546 unique (R_{int} = 0.1245, R_{sigma} = 0.1707) which were used in all calculations. The final R_1 was 0.0919 (I > 2σ(I)) and wR_2 was 0.3108 (all data).

Table 2 Fractional Atomic Coordinates (×10^4) and Equivalent Isotropic Displacement Parameters (Å^2×10^3) for SCY-CF3. U$_{eq}$ is defined as 1/3 of the trace of the orthogonalised U$_{IJ}$ tensor.

Atom	***x***	***y***	***z***	**U(eq)**
F1	1266(3)	13324(2)	6776.4(18)	106.3(8)
F2	1999(3)	13660.1(19)	5571(2)	83.1(8)
F3	-160(2)	12534.9(19)	5144(2)	77.4(8)
F4	441(4)	8022(2)	-2578(2)	109.2(12)
F5	-1525(3)	6643(2)	-3055(2)	102.9(9)
F6	112(3)	6261(2)	-3733.6(18)	101.8(9)
F7	3279(2)	8716.5(16)	2419.7(13)	52.8(6)
F8	962.1(18)	7571.9(16)	2057.8(13)	50.3(6)
N1	2835(3)	7912(2)	3594.5(18)	41.9(6)
N2	2619(3)	6583(2)	1641.2(19)	43.1(6)
N3	3554(3)	6220(2)	3085.0(19)	46.3(6)
C1	3411(3)	7157(3)	3824(2)	45.9(6)
C2	3918(4)	7657(3)	4988(2)	51.9(7)
C3	3671(3)	8679(3)	5437(2)	51.3(7)
C4	3018(3)	8850(3)	4583(2)	44.2(6)
C5	2566(3)	9844(3)	4784(2)	42.0(7)
C6	3296(3)	10909(3)	5802(2)	47.0(8)
C7	2847(3)	11851(3)	6080(2)	50.0(8)
C8	1678(3)	11795(3)	5394(2)	48.9(7)
C9	1388(4)	9815(3)	4086(3)	54.1(8)
C10	928(4)	10754(3)	4375(2)	51.6(8)
C11	1194(4)	12815(3)	5723(3)	55.7(6)
C12	3684(9)	5949(5)	5243(4)	157(3)
C13	4567(5)	7077(3)	5554(3)	80.8(10)
C14	5168(4)	7854(3)	6777(3)	57.5(9)
C15	4299(5)	8021(4)	7450(3)	78.0(13)

Table 2 Fractional Atomic Coordinates ($\times10^4$) and Equivalent Isotropic Displacement Parameters ($Å^2\times10^3$) for SCY-CF3. U_{eq} is defined as 1/3 of the trace of the orthogonalised U_{IJ} tensor.

Atom	*x*	*y*	*z*	U(eq)
C16	4864(4)	8690(4)	8590(3)	72.5(13)
C17	6321(5)	9199(3)	9057(3)	65.0(10)
C18	7199(5)	9062(4)	8403(3)	81.3(15)
C19	6635(5)	8393(4)	7272(3)	75.0(13)
C20	3164(3)	5938(3)	2045(2)	44.8(6)
C21	3125(3)	4876(3)	1133(2)	45.6(6)
C22	3673(4)	3970(3)	1239(3)	52.3(8)
C23	5249(4)	4499(4)	1867(3)	77.0(15)
C24	3257(3)	2869(3)	132(2)	44.2(8)
C25	1817(3)	2109(3)	-376(3)	52.5(10)
C26	1417(4)	1070(3)	-1363(3)	56.5(10)
C27	2443(4)	742(3)	-1837(3)	55.9(10)
C28	3876(4)	1482(3)	-1344(2)	55.1(10)
C29	4268(3)	2532(3)	-374(2)	49.4(9)
C30	2532(3)	4906(3)	221(2)	48.4(7)
C31	2205(3)	5924(3)	509(2)	43.1(6)
C32	1590(3)	6264(3)	-252(2)	43.1(6)
C33	1838(3)	7402(3)	-72(2)	48.1(7)
C34	1290(3)	7638(3)	-872(2)	48.8(8)
C35	455(3)	6691(3)	-1912(2)	45.9(7)
C36	714(3)	5310(3)	-1320(2)	44.9(8)
C37	176(4)	5566(3)	-2115(2)	50.1(7)
C38	-104(4)	6923(3)	-2794(3)	61.3(7)
B1	2400(4)	7733(3)	2410(3)	45.1(6)

Table 3 Anisotropic Displacement Parameters ($Å^2\times10^3$) for SCY-CF3. The Anisotropic displacement factor exponent takes the form: $-2\pi^2[h^2a^{*2}U_{11}+2hka^*b^*U_{12}+\dots]$.

Atom	U_{11}	U_{22}	U_{33}	U_{23}	U_{13}	U_{12}
F1	182.2(16)	122.0(13)	65.6(8)	44.3(9)	61.1(9)	122.0(9)
F2	77.4(12)	64.6(9)	125.3(13)	56.4(7)	34.7(10)	33.1(8)
F3	65.7(9)	71.2(11)	99.8(13)	36.3(9)	24.1(8)	42.9(7)
F4	148(3)	82.5(9)	86.6(12)	57.3(7)	-6.4(15)	20.9(13)
F5	65.1(9)	159.1(16)	120.0(14)	98.7(10)	16.7(10)	46.7(10)
F6	142.6(17)	137.9(15)	64.8(9)	59.2(9)	42.5(9)	87.6(11)
F7	63.5(9)	57.4(8)	45.6(7)	25.9(6)	24.9(7)	28.0(7)

Table 3 Anisotropic Displacement Parameters ($\text{Å}^2\times10^3$) for SCY-CF3. The Anisotropic displacement factor exponent takes the form: $-2\pi^2[h^2a^{*2}U_{11}+2hka^*b^*U_{12}+\ldots]$.

Atom	U_{11}	U_{22}	U_{33}	U_{23}	U_{13}	U_{12}
F8	47.8(6)	63.2(9)	42.3(8)	18.8(7)	17.0(6)	34.7(6)
N1	43.3(10)	52.9(8)	41.9(6)	23.8(5)	22.7(7)	29.4(6)
N2	42.8(10)	53.6(8)	45.2(7)	26.3(5)	20.9(7)	28.0(6)
N3	52.1(11)	59.9(10)	44.1(6)	28.0(6)	23.8(7)	36.5(7)
C1	52.3(12)	58.4(8)	45.3(7)	28.8(6)	26.2(8)	35.1(6)
C2	57.9(13)	68.8(8)	45.1(8)	29.7(6)	22.1(9)	40.3(7)
C3	59.8(14)	65.8(9)	42.9(9)	28.1(6)	25.1(9)	36.6(8)
C4	44.1(12)	55.6(8)	38.4(7)	20.7(6)	20.1(8)	26.6(7)
C5	44.0(10)	52.3(8)	33.3(9)	17.2(7)	20.4(7)	24.8(6)
C6	41.0(12)	55.1(9)	39.5(12)	15.7(8)	8.9(10)	25.0(7)
C7	52.2(11)	50.9(9)	41.2(12)	14.0(8)	14.1(8)	25.8(7)
C8	57.3(11)	60.4(9)	42.4(10)	25.0(7)	24.1(8)	37.0(7)
C9	59.1(11)	67.6(10)	42.6(11)	22.8(8)	19.4(8)	39.0(7)
C10	58.5(13)	66.4(9)	39.5(11)	23.5(9)	19.8(10)	39.2(7)
C11	65.4(10)	56.6(8)	58.0(8)	27.3(7)	29.4(7)	36.8(7)
C12	270(6)	92.3(15)	45(2)	31.0(16)	-24(3)	17(2)
C13	135(2)	73.2(10)	47.1(10)	22.9(7)	19.5(12)	73.9(9)
C14	83.7(10)	57.5(15)	45.7(9)	24.9(10)	21.6(7)	47.1(11)
C15	79.6(14)	107(3)	50.2(9)	27.0(13)	21.6(8)	57.5(14)
C16	83.8(12)	92(2)	50.1(10)	27.0(14)	30.8(11)	52.5(14)
C17	87.4(10)	72.1(19)	47.2(11)	33.0(11)	21.1(8)	39.2(13)
C18	77.2(15)	94(3)	60.3(9)	32.4(13)	23.3(8)	19.7(18)
C19	82.9(13)	90(2)	57.9(10)	37.4(13)	28.3(11)	34.9(17)
C20	46.0(12)	60.2(8)	45.8(6)	30.0(5)	23.9(7)	33.1(7)
C21	45.5(12)	55.5(8)	48.3(7)	26.6(6)	27.0(7)	28.1(7)
C22	61.9(11)	59.5(9)	41.6(11)	23.2(7)	16.7(10)	33.9(8)
C23	68.8(13)	71(2)	74(2)	17.2(18)	5.1(14)	43.2(14)
C24	47.9(9)	58.0(13)	38.4(10)	25.8(8)	16.9(7)	31.1(8)
C25	44.1(11)	68.3(14)	51.8(12)	26.0(10)	21.7(10)	32.5(10)
C26	45.4(11)	64.2(15)	54.3(12)	22.9(10)	15.2(8)	22.6(10)
C27	54.0(9)	70.2(17)	42.9(13)	22.3(12)	13.0(8)	32.5(9)
C28	52.3(11)	77.4(15)	38.1(11)	20.6(10)	22.0(10)	36.7(10)
C29	42.3(10)	66.6(14)	39.6(10)	22.4(9)	15.3(8)	25.4(9)
C30	48.8(13)	58.0(9)	48.8(8)	26.1(6)	25.0(9)	29.2(7)
C31	35.6(11)	55.2(8)	45.5(7)	24.6(6)	20.3(8)	22.7(7)
C32	40.3(12)	55.6(7)	39.2(8)	20.2(5)	20.0(8)	26.9(8)
C33	49.3(13)	59.3(8)	45.9(8)	25.4(6)	22.2(9)	31.5(8)

Table 3 Anisotropic Displacement Parameters (Å^2×10^3) for SCY-CF3. The Anisotropic displacement factor exponent takes the form: $-2\pi^2[h^2a^{*2}U_{11}+2hka^*b^*U_{12}+\ldots]$.

Atom	U_{11}	U_{22}	U_{33}	U_{23}	U_{13}	U_{12}
C34	44.2(14)	55.9(12)	46.2(8)	22.3(6)	13.7(9)	23.1(10)
C35	42.4(13)	59.6(8)	43.0(8)	26.3(6)	16.3(9)	25.6(9)
C36	46.6(14)	49.2(11)	41.2(8)	20.3(6)	15.0(8)	23.3(9)
C37	50.6(15)	59.2(8)	42.3(9)	23.8(6)	12.3(10)	25.9(9)
C38	63.2(10)	75.3(9)	57.2(8)	40.2(6)	14.2(8)	31.7(9)
B1	46.1(9)	60.1(9)	45.5(8)	28.8(6)	23.3(8)	33.4(7)

Table 4 Bond Lengths for SCY-CF3.

Atom	Atom	Length/Å	Atom	Atom	Length/Å
F1	C11	1.325(4)	C12	C13	1.378(7)
F2	C11	1.338(5)	C13	C14	1.499(5)
F3	C11	1.339(4)	C14	C15	1.373(6)
F4	C38	1.312(5)	C14	C19	1.372(6)
F5	C38	1.324(5)	C15	C16	1.393(5)
F6	C38	1.331(5)	C16	C17	1.358(6)
F7	B1	1.383(5)	C17	C18	1.361(7)
F8	B1	1.379(4)	C18	C19	1.382(5)
N1	C1	1.413(5)	C20	C21	1.439(4)
N1	C4	1.365(4)	C21	C22	1.512(6)
N1	B1	1.561(5)	C21	C30	1.358(5)
N2	C20	1.397(5)	C22	C23	1.498(5)
N2	C31	1.382(4)	C22	C24	1.516(4)
N2	B1	1.554(5)	C24	C25	1.393(4)
N3	C1	1.304(4)	C24	C29	1.387(5)
N3	C20	1.316(4)	C25	C26	1.386(4)
C1	C2	1.429(4)	C26	C27	1.374(6)
C2	C3	1.349(5)	C27	C28	1.381(4)
C2	C13	1.521(6)	C28	C29	1.381(4)
C3	C4	1.421(5)	C30	C31	1.391(5)
C4	C5	1.446(5)	C31	C32	1.456(5)
C5	C6	1.423(4)	C32	C33	1.385(5)
C5	C9	1.400(5)	C32	C36	1.430(3)
C6	C7	1.370(5)	C33	C34	1.378(6)
C7	C8	1.367(5)	C34	C35	1.396(4)
C8	C10	1.412(4)	C35	C37	1.355(5)
C8	C11	1.480(6)	C35	C38	1.478(6)

Table 4 Bond Lengths for SCY-CF3.

Atom	Atom	Length/Å	Atom	Atom	Length/Å
C9	C10	1.373(6)	C36	C37	1.386(5)

Table 5 Bond Angles for SCY-CF3.

Atom	Atom	Atom	Angle/°	Atom	Atom	Atom	Angle/°
C1	N1	B1	121.8(3)	N2	C20	C21	108.9(3)
C4	N1	C1	106.7(3)	N3	C20	N2	125.3(3)
C4	N1	B1	130.4(3)	N3	C20	C21	125.7(4)
C20	N2	B1	122.0(3)	C20	C21	C22	124.6(3)
C31	N2	C20	106.7(3)	C30	C21	C20	105.3(3)
C31	N2	B1	130.9(3)	C30	C21	C22	130.0(3)
C1	N3	C20	119.5(3)	C21	C22	C24	111.2(3)
N1	C1	C2	108.4(3)	C23	C22	C21	111.7(3)
N3	C1	N1	124.7(3)	C23	C22	C24	114.7(3)
N3	C1	C2	126.7(4)	C25	C24	C22	119.7(3)
C1	C2	C13	124.0(3)	C29	C24	C22	122.7(3)
C3	C2	C1	106.8(4)	C29	C24	C25	117.5(3)
C3	C2	C13	129.2(3)	C26	C25	C24	120.8(3)
C2	C3	C4	109.1(3)	C27	C26	C25	120.6(3)
N1	C4	C3	108.9(3)	C26	C27	C28	119.3(3)
N1	C4	C5	127.8(3)	C29	C28	C27	120.0(3)
C3	C4	C5	123.2(3)	C28	C29	C24	121.7(3)
C6	C5	C4	118.0(3)	C21	C30	C31	110.6(3)
C9	C5	C4	124.9(2)	N2	C31	C30	108.5(3)
C9	C5	C6	116.9(3)	N2	C31	C32	125.6(3)
C7	C6	C5	120.9(3)	C30	C31	C32	125.8(3)
C8	C7	C6	121.2(3)	C33	C32	C31	127.0(2)
C7	C8	C10	119.5(3)	C33	C32	C36	117.4(3)
C7	C8	C11	120.2(3)	C36	C32	C31	115.6(3)
C10	C8	C11	120.3(3)	C34	C33	C32	122.8(3)
C10	C9	C5	122.0(3)	C33	C34	C35	118.7(4)
C9	C10	C8	119.5(3)	C34	C35	C38	119.6(4)
F1	C11	F2	106.3(3)	C37	C35	C34	120.1(4)
F1	C11	F3	107.4(3)	C37	C35	C38	120.2(3)
F1	C11	C8	112.2(4)	C37	C36	C32	119.0(3)
F2	C11	F3	104.6(4)	C35	C37	C36	122.0(3)
F2	C11	C8	112.3(3)	F4	C38	F5	105.9(4)
F3	C11	C8	113.4(3)	F4	C38	F6	106.4(4)

Table 5 Bond Angles for SCY-CF3.

Atom	Atom	Atom	Angle/°	Atom	Atom	Atom	Angle/°
C12	C13	C2	114.2(4)	F4	C38	C35	115.3(3)
C12	C13	C14	112.9(4)	F5	C38	F6	103.7(3)
C14	C13	C2	112.9(3)	F5	C38	C35	112.4(4)
C15	C14	C13	122.3(4)	F6	C38	C35	112.2(4)
C15	C14	C19	117.2(3)	F7	B1	N1	107.9(2)
C19	C14	C13	120.4(4)	F7	B1	N2	112.3(3)
C14	C15	C16	122.2(4)	F8	B1	F7	110.7(3)
C17	C16	C15	119.3(4)	F8	B1	N1	111.6(3)
C16	C17	C18	119.4(3)	F8	B1	N2	107.7(2)
C17	C18	C19	121.1(4)	N2	B1	N1	106.5(3)
C14	C19	C18	120.8(4)				

Table 6 Torsion Angles for SCY-CF3.

A	B	C	D	Angle/°	A	B	C	D	Angle/°
N1	C1	C2	C3	-0.8(4)	C17	C18	C19	C14	0.5(9)
N1	C1	C2	C13	177.9(3)	C19	C14	C15	C16	-1.0(8)
N1	C4	C5	C6	-157.2(3)	C20	N2	C31	C30	-1.7(3)
N1	C4	C5	C9	27.8(6)	C20	N2	C31	C32	-179.3(3)
N2	C20	C21	C22	177.8(3)	C20	N2	B1	F7	115.7(3)
N2	C20	C21	C30	-1.4(4)	C20	N2	B1	F8	-122.1(3)
N2	C31	C32	C33	29.2(5)	C20	N2	B1	N1	-2.2(4)
N2	C31	C32	C36	-155.1(3)	C20	N3	C1	N1	1.1(5)
N3	C1	C2	C3	173.9(3)	C20	N3	C1	C2	-172.8(3)
N3	C1	C2	C13	-7.4(6)	C20	C21	C22	C23	-59.6(5)
N3	C20	C21	C22	-6.5(5)	C20	C21	C22	C24	170.8(3)
N3	C20	C21	C30	174.3(3)	C20	C21	C30	C31	0.3(4)
C1	N1	C4	C3	-1.6(4)	C21	C22	C24	C25	-71.0(5)
C1	N1	C4	C5	-178.0(3)	C21	C22	C24	C29	113.7(4)
C1	N1	B1	F7	-116.4(3)	C21	C30	C31	N2	0.9(4)
C1	N1	B1	F8	121.8(3)	C21	C30	C31	C32	178.4(3)
C1	N1	B1	N2	4.4(4)	C22	C21	C30	C31	-178.9(3)
C1	N3	C20	N2	1.4(5)	C22	C24	C25	C26	-177.1(4)
C1	N3	C20	C21	-173.6(3)	C22	C24	C29	C28	175.3(4)
C1	C2	C3	C4	-0.2(4)	C23	C22	C24	C25	161.0(4)
C1	C2	C13	C12	-56.0(6)	C23	C22	C24	C29	-14.3(6)
C1	C2	C13	C14	173.2(4)	C24	C25	C26	C27	3.0(7)
C2	C3	C4	N1	1.1(4)	C25	C24	C29	C28	-0.1(6)

Table 6 Torsion Angles for SCY-CF3.

A	B	C	D	Angle/˚	A	B	C	D	Angle/˚
C2	C3	C4	C5	177.7(3)	C25	C26	C27	C28	-2.8(7)
C2	C13	C14	C15	77.0(6)	C26	C27	C28	C29	1.1(7)
C2	C13	C14	C19	-105.8(5)	C27	C28	C29	C24	0.3(7)
C3	C2	C13	C12	122.3(5)	C29	C24	C25	C26	-1.5(6)
C3	C2	C13	C14	-8.5(6)	C30	C21	C22	C23	119.4(4)
C3	C4	C5	C6	26.8(5)	C30	C21	C22	C24	-10.1(5)
C3	C4	C5	C9	-148.2(4)	C30	C31	C32	C33	-148.0(4)
C4	N1	C1	N3	-173.4(3)	C30	C31	C32	C36	27.7(5)
C4	N1	C1	C2	1.4(4)	C31	N2	C20	N3	-173.8(3)
C4	N1	B1	F7	49.8(4)	C31	N2	C20	C21	1.9(3)
C4	N1	B1	F8	-72.0(4)	C31	N2	B1	F7	-72.9(4)
C4	N1	B1	N2	170.6(3)	C31	N2	B1	F8	49.3(5)
C4	C5	C6	C7	-174.8(3)	C31	N2	B1	N1	169.2(3)
C4	C5	C9	C10	173.5(4)	C31	C32	C33	C34	175.1(3)
C5	C6	C7	C8	0.6(6)	C31	C32	C36	C37	-175.4(3)
C5	C9	C10	C8	1.4(6)	C32	C33	C34	C35	-0.3(5)
C6	C5	C9	C10	-1.6(6)	C32	C36	C37	C35	0.0(5)
C6	C7	C8	C10	-0.8(6)	C33	C32	C36	C37	0.7(5)
C6	C7	C8	C11	178.6(4)	C33	C34	C35	C37	1.1(5)
C7	C8	C10	C9	-0.2(6)	C33	C34	C35	C38	-178.0(3)
C7	C8	C11	F1	-40.1(5)	C34	C35	C37	C36	-0.9(6)
C7	C8	C11	F2	79.6(5)	C34	C35	C38	F4	11.2(6)
C7	C8	C11	F3	-162.0(4)	C34	C35	C38	F5	-110.3(4)
C9	C5	C6	C7	0.6(5)	C34	C35	C38	F6	133.2(3)
C10	C8	C11	F1	139.3(4)	C36	C32	C33	C34	-0.6(5)
C10	C8	C11	F2	-101.0(4)	C37	C35	C38	F4	-167.9(4)
C10	C8	C11	F3	17.4(5)	C37	C35	C38	F5	70.6(5)
C11	C8	C10	C9	-179.6(4)	C37	C35	C38	F6	-45.8(5)
C12	C13	C14	C15	-54.4(7)	C38	C35	C37	C36	178.1(4)
C12	C13	C14	C19	122.8(6)	B1	N1	C1	N3	-4.3(5)
C13	C2	C3	C4	-178.7(4)	B1	N1	C1	C2	170.5(3)
C13	C14	C15	C16	176.3(5)	B1	N1	C4	C3	-169.4(3)
C13	C14	C19	C18	-176.7(5)	B1	N1	C4	C5	14.2(5)
C14	C15	C16	C17	0.2(8)	B1	N2	C20	N3	-0.5(5)
C15	C14	C19	C18	0.7(8)	B1	N2	C20	C21	175.2(3)
C15	C16	C17	C18	1.1(8)	B1	N2	C31	C30	-174.2(3)
C16	C17	C18	C19	-1.4(8)	B1	N2	C31	C32	8.3(5)

Table 7 Hydrogen Atom Coordinates (Å×10^4) and Isotropic Displacement Parameters (Å^2×10^3) for SCY-CF3.

Atom	*x*	*y*	*z*	U(eq)
H3	3897.27	9200.77	6201.33	62
H6	4106.45	10967.79	6296.6	56
H7	3357.37	12555.43	6761.53	60
H9	891.44	9123.81	3391.73	65
H10	112.56	10704.62	3892.23	62
H12A	2676.6	5901.71	5131.61	235
H12B	3964.02	5756.41	5818.65	235
H12C	3785.02	5385.59	4556.43	235
H13	5423.07	6984.7	5293.35	97
H15	3279.08	7668.88	7127.26	94
H16	4237.5	8788.54	9035.66	87
H17	6723.42	9645.99	9833.31	78
H18	8218.12	9433.18	8728.67	98
H19	7270.3	8304.98	6832.56	90
H22	3150.36	3719.63	1691.75	63
H23A	5801.71	4856.72	1507.52	116
H23B	5578.43	3879.45	1885.65	116
H23C	5398.11	5106.22	2619.12	116
H25	1100.78	2304.49	-40.79	63
H26	425.03	580.31	-1715.77	68
H27	2169.04	12.22	-2497.06	67
H28	4590.91	1270.72	-1671.98	66
H29	5256.53	3035.5	-45.56	59
H30	2362.83	4313.3	-511.97	58
H33	2410.12	8047.43	634.12	58
H34	1476.45	8429.6	-719.68	59
H36	504.54	4514.07	-1481.58	54
H37	-406.88	4932.15	-2824.55	60

6 References

[1] M.J.T. Frisch, G. W.; Schlegel, H. B.; Scuseria, G. E.; Robb, M. A.; Cheeseman, J. R.; Scalmani, G.; Barone, V.; Mennucci, B.; Petersson, G. A.; Nakatsuji, H.; Caricato, M.; Li, X.; Hratchian, H. P.; Izmaylov, A. F.; Bloino, J.; Zheng, G.; Sonnenberg, J. L.; Hada, M.; Ehara, M.; Toyota, K.; Fukuda, R.; Hasegawa, J.; Ishida, M.; Nakajima, T.; Honda, Y.; Kitao, O.; Nakai, H.; Vreven, T.; Montgomery, J. A., Jr.; Peralta, J. E.; Ogliaro, F.; Bearpark, M.; Heyd, J. J.; Brothers, E.; Kudin, K. N.; Staroverov, V. N.; Keith, T.; Kobayashi, R.; Normand, J.; Raghavachari, K.; Rendell, A.; Burant, J. C.; Iyengar, S. S.; Tomasi, J.; Cossi, M.; Rega, N.; Millam, J. M.; Klene, M.; Knox, J. E.; Cross, J. B.; Bakken, V.; Adamo, C.; Jaramillo, J.; Gomperts, R.; Stratmann, R. E.; Yazyev, O.; Austin, A. J.; Cammi, R.; Pomelli, C.; Ochterski, J. W.; Martin, R. L.; Morokuma, K.; Zakrzewski, V. G.; Voth, G. A.; Salvador, P.; Dannenberg, J. J.; Dapprich, S.; Daniels, A. D.; Farkas, O.; Foresman, J. B.; Ortiz, J. V.; Cioslowski, J.; Fox, D. J., Gaussian 09, revision D01, (2013).

[2] A.D. Becke, Density-Functional Thermochemistry .3. The Role Of Exact Exchange, J Chem Phys, 98(1993) 5648-52.

[3] C.T. Lee, W.T. Yang, R.G. Parr, Development Of the Colle-Salvetti Correlation-Energy Formula into a Functional Of the Electron-Density, Phys Rev B, 37(1988) 785-9.

[4] S. Grimme, S. Ehrlich, L. Goerigk, Effect of the damping function in dispersion corrected density functional theory, J Comput Chem, 32(2011) 1456-65.

[5] V. Barone, M. Cossi, J. Tomasi, A new definition of cavities for the computation of solvation free energies by the polarizable continuum model, J Chem Phys, 107(1997) 3210-21.

[6] J. Tomasi, B. Mennucci, R. Cammi, Quantum mechanical continuum solvation models, Chem Rev, 105(2005) 2999-3093.